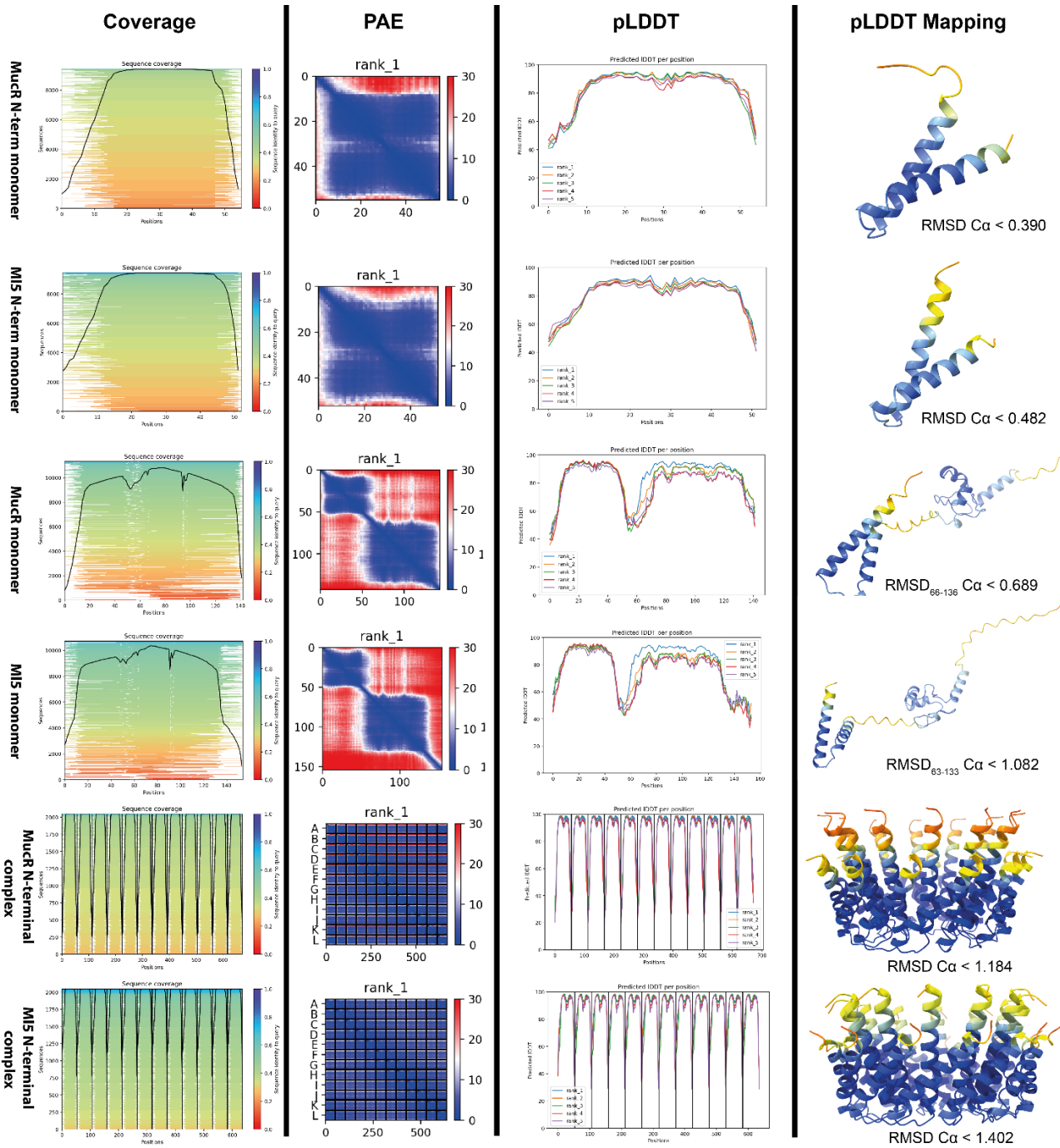


## Supplementary Data

<b>Primers used for PCR</b>	
PRIMER	SEQUENCE 5'-3'
1	ATCGCATATGACCGAAGAAACCGAGAGCAAAG
2	TATCGAATTCTCAGGCTGCCGCTTTCTTGCGGGC
3	CTGTGAAGCGCCTGGGGCTGCCGGCCAGATCCACATCGCATTGAAAG
4	CTGGCCGGCAGCCCCAGGCGCTTACCGACGGGAACCGGATTGTTGCAAAC
5	GCCTCTAGACATGAGCACCGACGTCAGCAGTG
6	GTCCTGGGAGTGCCGGGAGAGCATCAGCATG
<b>Oligonucleotides used for Bridging Assays</b>	
OLIGONUCLEOTIDE	SEQUENCE OF SINGLE STRAND (5'-3')
<i>mucR</i> promoter	TCTCAATTTTCTTGCGGTGCCCTGTTTAATATCATTTTATTTGTCGATCTAAG AAGAGTTGCCTATTATTAATGTAATATGGTTTGACAATTCTATTGCAAATGG CATCGTCAATTGATATTTCCATAAGGGATCGAGTTGGGCCGGATTATGAAA TACGCAGCGGCGGCAAGGGGTGGGTTGCCATTGTCAGCCGCTGCGCGGAC AACAAAAAATTA AAAAAGGAAA ACTT
babR60 (stretched by 26 amino acids; see Methods)	AATTTAGAATGAAGTTATATTCAATATAAAAAGTAGAATTTGAAAATCGCTA ATTATGATAATTTAGAATGAAGTTATATTCAATA

**Supplementary Table 1.** Primer sequences used for PCR and oligonucleotide sequences tested in bridging assays are reported.

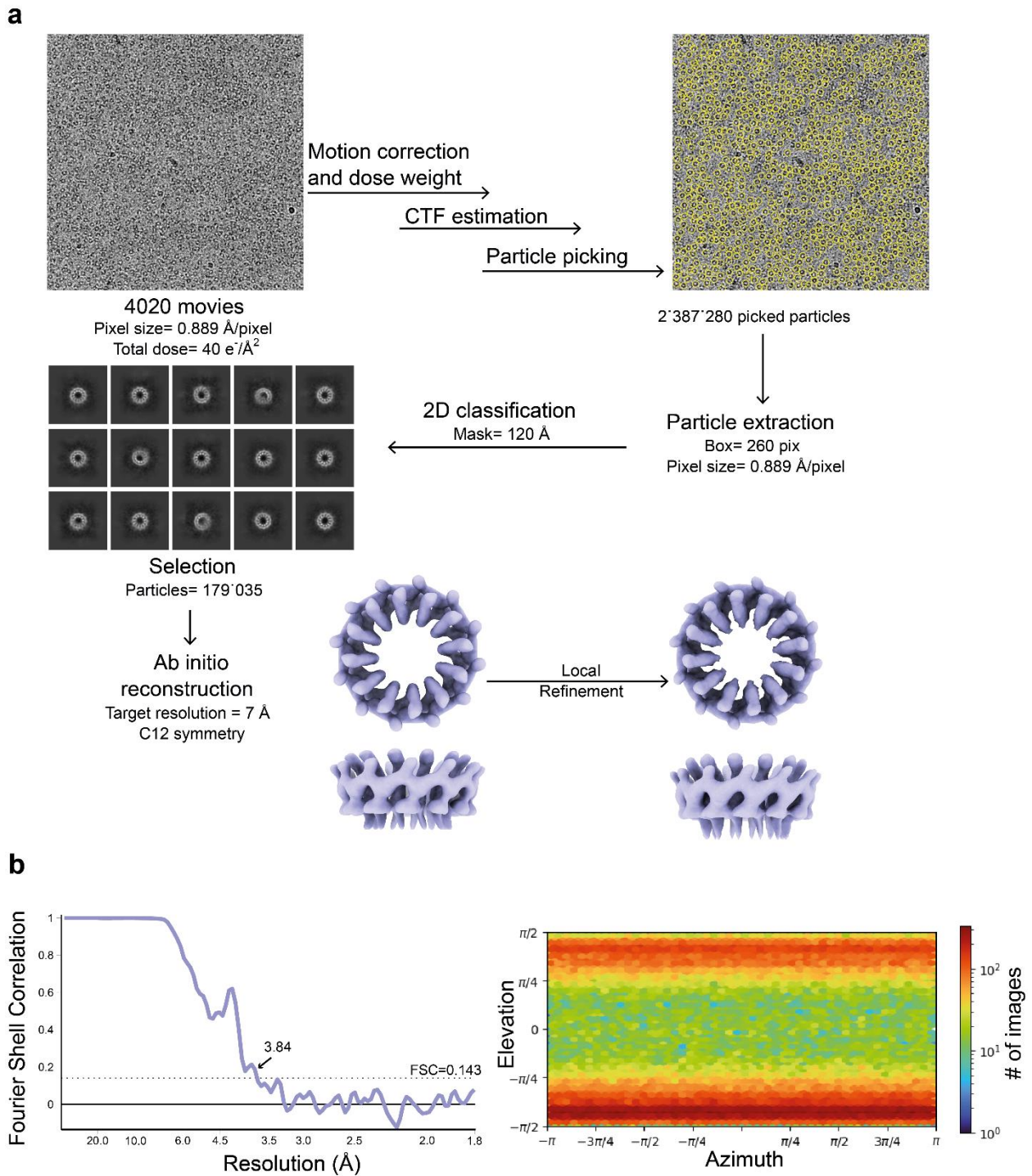


**Supplementary Table 2: AlphaFold metrics.** Sequence coverage, PAE map, per-residues pLDDT and pLDDT mapped on the best model are reported. Maximum  $C\alpha$  RMSD for the five AF2 models obtained for every query is also indicated.

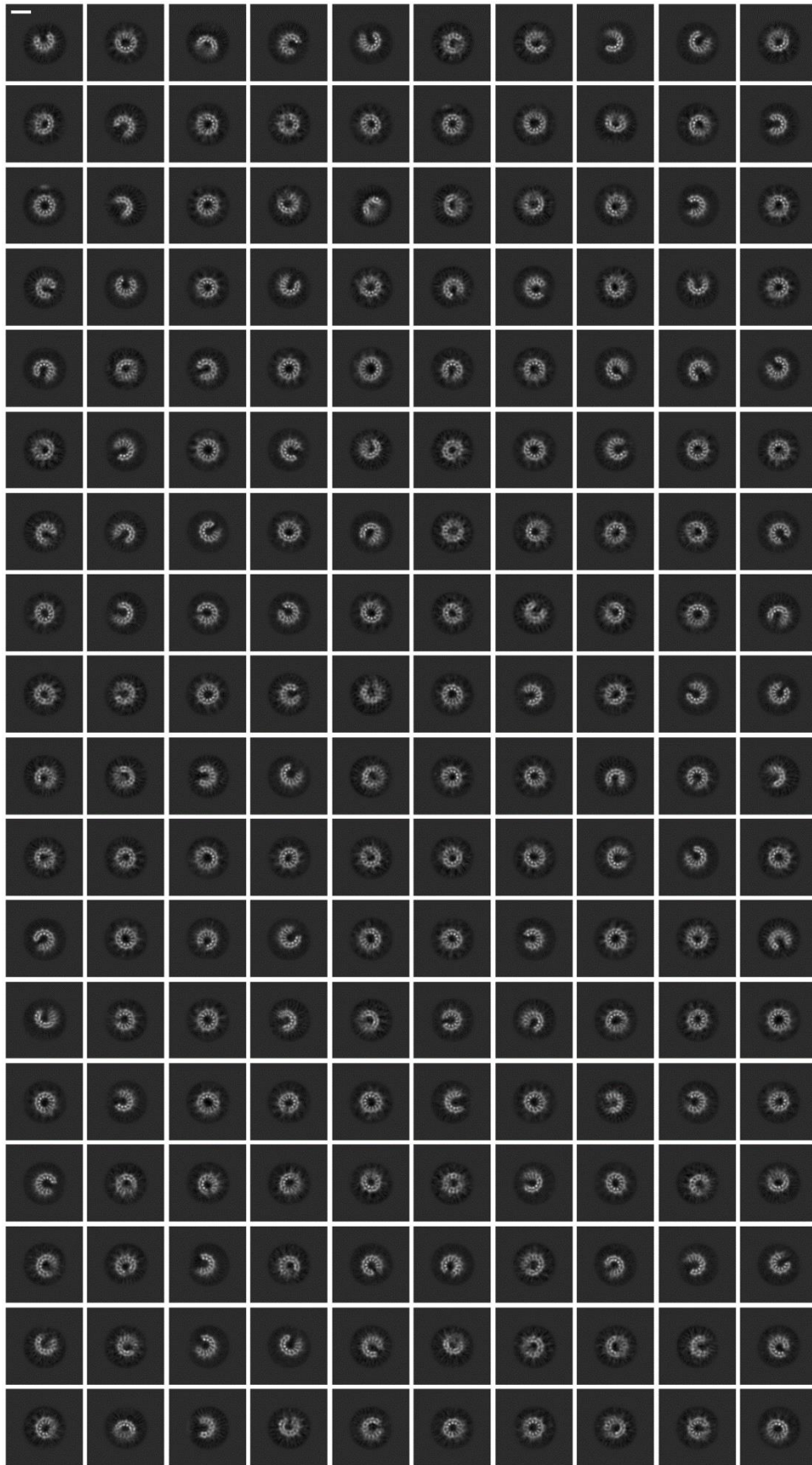
Residue #	Residue type	Chemical Shift (ppm)			
		H <sub>N</sub>	N	C <sub>α</sub>	C <sub>β</sub>
58	V	-	-	60.20	30.06
59	V	8.36	125.61	59.53	30.22
60	V	8.31	125.57	59.36	30.22
61	E	8.44	125.75	53.32	28.14
62	K	8.42	124.80	51.45	-
63	P	-	-	59.92	29.42
64	K	8.65	122.96	50.73	-
65	P	-	-	59.72	29.74
66	A	8.53	121.84	52.04	17.03
67	V	7.04	106.00	55.25	33.02
68	N	8.25	119.50	48.71	-
69	P	-	-	63.07	30.06
70	K	8.43	116.94	55.35	29.42
71	K	8.23	119.33	51.80	29.82
72	S	7.62	112.60	57.12	62.35
73	V	8.27	123.36	60.84	29.58
74	H	8.65	129.33	51.32	28.86
75	D	8.11	119.08	55.54	37.18
76	D	9.03	111.90	51.41	40.45
77	Y	6.98	113.50	54.38	36.62
78	I	9.41	118.66	56.88	38.77
79	V	9.08	126.85	58.68	30.25
80	C	9.28	129.87	57.25	26.78
81	L	9.15	130.44	53.95	36.22
82	E	9.08	117.33	55.39	28.22
83	D	6.74	109.12	51.60	40.88
84	G	8.76	111.12	43.43	-
85	K	8.66	122.09	53.57	31.18
86	K	7.48	117.80	53.06	31.98
87	F	8.94	118.41	55.06	41.25
88	K	8.82	122.08	56.84	29.74
89	S	7.66	108.49	52.70	60.63
90	L	8.74	129.33	54.14	40.69
91	K	7.96	117.38	58.23	30.07
92	R	8.03	116.92	55.80	27.34
93	H	7.39	117.85	55.06	25.27
94	L	8.21	119.79	55.46	38.48
95	V	6.83	114.37	62.36	29.10
96	T	7.56	110.71	60.97	66.40
97	H	7.56	122.66	50.83	24.71
98	Y	7.71	115.57	55.97	33.18
99	N	7.99	112.39	51.79	34.86
100	M	7.16	120.43	54.58	32.06
101	T	7.98	113.60	56.50	-
102	P	-	-	63.95	30.06

103	E	8.92	115.45	58.09	26.22
104	Q	7.91	119.95	55.87	26.54
105	Y	8.56	122.83	59.64	36.70
106	R	8.62	115.88	57.41	27.26
107	E	7.80	116.74	56.31	27.34
108	K	8.15	120.60	56.31	29.66
109	W	7.15	115.03	52.85	27.02
110	D	7.59	118.01	52.69	36.62
111	L	8.62	116.96	50.25	39.65
112	D	8.60	122.53	50.44	-
113	P	-	-	62.59	29.50
114	N	8.54	112.90	49.59	35.90
115	Y	8.32	126.61	54.67	30.38
116	P	-	-	60.58	-
117	M	8.10	109.44	49.92	33.74
118	V	7.53	117.90	57.35	32.78
119	A	8.81	129.56	48.45	-
120	P	-	-	63.63	30.06
121	N	9.04	114.46	51.97	34.62
122	Y	8.04	120.39	56.40	36.22
123	A	7.94	123.29	51.07	16.31
124	A	8.13	121.28	51.00	16.23
125	A	7.94	121.76	51.06	16.23
126	R	8.13	118.49	54.48	27.66
127	S	8.10	115.78	56.84	60.88
128	R	8.12	122.11	54.73	27.90
129	L	7.96	121.30	53.14	39.57
130	A	8.03	123.45	50.47	16.39
131	K	8.06	119.56	54.15	30.30
132	K	8.17	121.60	54.03	30.06
133	M	8.32	120.46	52.94	30.22
134	G	8.33	109.43	42.76	-
135	L	8.18	121.39	52.65	39.78
136	G	8.49	109.44	42.61	-
137	R	8.09	120.28	53.08	28.30
138	K	8.45	124.37	51.55	-
139	P	-	-	60.60	29.66
140	K	8.39	120.91	54.00	30.38
141	D	8.33	121.47	51.76	38.53
142	A	7.78	128.95	51.21	-

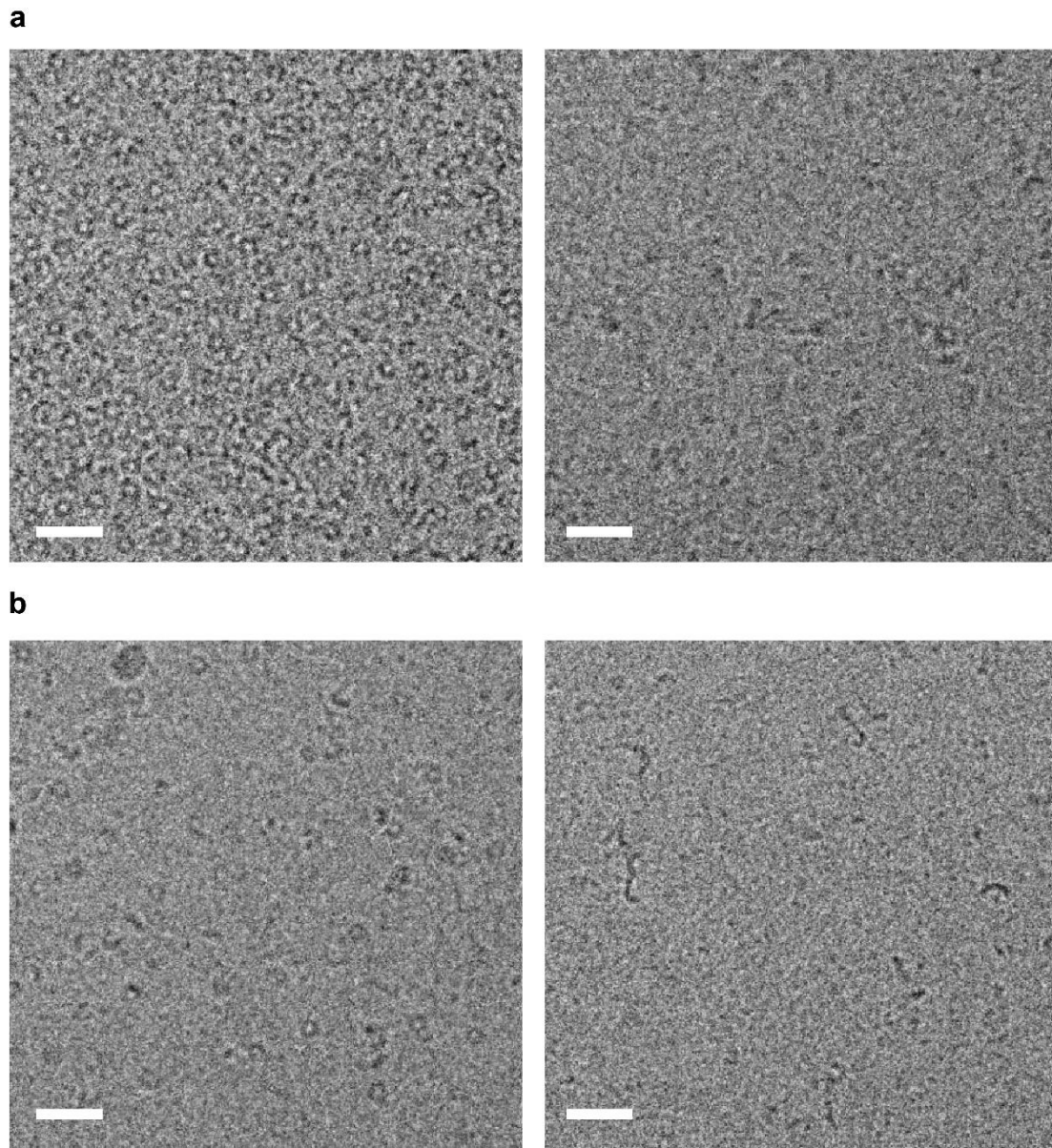
**Supplementary Table 3: NMR Chemical Shifts.** Assigned chemical shifts of backbone H<sub>N</sub>, N, C<sub>α</sub>, and C<sub>β</sub> nuclei of MucR DBD.



**Supplementary Figure 1. Cryo-EM processing workflow.** (a) The workflow is described in the methods section. Representative micrographs with and without the particle coordinates are shown. The 2D averages of the final set of particles are displayed in the selection. Two representative views of the *ab initio* reconstruction and the final reconstruction are shown. Important processing parameters are labeled below each processing step. (b) On the left, Fourier Shell Correlation (FSC) plot for the final reconstruction. The FSC=0.143 cut-off is marked as dashed line. The resolution limit for an FSC=0.143 is highlighted with an arrow. On the right, viewing direction distribution for particle projections. Heat map shows number of particles for each viewing angle.



**Supplementary Figure 2.** Complete set of Cryo-EM 2D averages after the second 2D classification. The 2D class averages are ordered according to the number of particles averaged within the class. The scale bar inserted in the first class represents 6 nm.



**Supplementary Figure 3. Cryo-EM images of MucR and MI5. (a)** Images of wild-type MucR (left) and MucR<sup>L36L39I40A</sup> (right). **(b)** Images of wild-type MI5 (left) and MI5<sup>L34L37I38A</sup> (right). The white scale bars represent 20 nm.

```

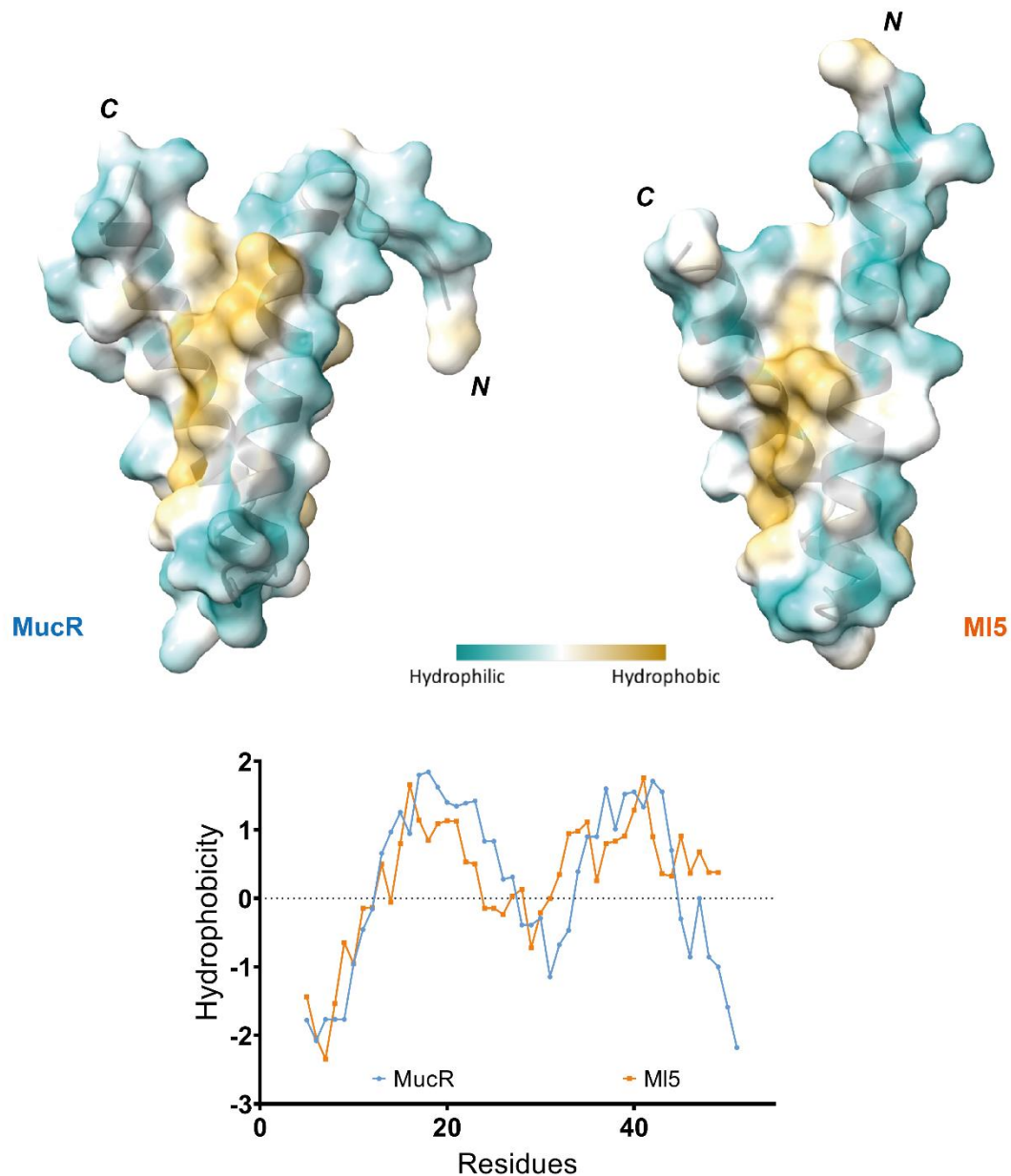
MucR_Babortus      -MENLETNDESTELLSSLTADVVAAYVGNNSIRAGELPVLIAEVHAAFKRRHVEREEAPVV
MucR_Bmelitensis  -MENLETNDESTELLSSLTADVVAAYVGNNSIRAGELPVLIAEVHAAFKRRHVEREEAPVV
M12_Mloti          -MDIVETPSRNNDALELTADVVAAYVSNNPVVPVGEPLNLI SDVHAALGRVGGTAEQPPA
MucR_Smeliloti    --MTETSLGTSNELLVLTAEI VAAVSNHVVPVAELPTLIADVHSALNNTTAPAPVVVP
Ros_Atumefaciens  --MTETAYGNAQDLLVELTADIVAAVSNHVVPVTELPGLISDVHTALSGETSAPASVAVN
M11_Mloti         ---MTEEADKNIDTLELTADVVSAYVSNNPVVPVGDLPALIGQVHAALKGTAG-FVSAAK
M15_Mloti         ---MTEETESKADNLIELTAHVVSAYVSNNPVVPVGEPLGLIGQIHIALKGTAG-GAAPEK
M13_Mloti         ---MKELSNIEDKTVIELTADIVSAYVGNNPPLPASGLPDLIASVSASVRKLAG--AVVVE
M14_Mloti         MPLRRKPLTDENINLIELTADIVSAYVSNNPVVPVASLPDLIHSVNL SLSKVGR--PAEPE
MucR2_Crescentus  -----MEDQSDLIEMTAGIVSAYVGNNVVSTADLPALIKQVHAALANVGAP-DAEAAA
MucR1_Crescentus  -----MEDKATLIELTAEIVANYVANNSTPVSELPALIRATHDALAGIGSPAPTVE
                  :::* * : * * . * : . * * * * .

MucR_Babortus      VEKPKPAVNPKKSVDHDIYVCLLEDGKKFKSLKRHLVTHYNMTPEQYREKWDLDPNYPMVA
MucR_Bmelitensis  VEKPKPAVNPKKSVDHDIYVCLLEDGKKFKSLKRHLVTHYNMTPEQYREKWDLDPNYPMVA
M12_Mloti         D-KQKPAVNPKRSVDHDIYVCLLEDGKKFKSLKRHLMTHYDLTPDQYREKWNLDPSYPMVA
MucR_Smeliloti    VEKPKPAVSVRKSVDQDITCLECGGTFKSLKRHLMTHHNLSPPEYRDKWDLPADYPMVA
Ros_Atumefaciens  VEKQKPAVSVRKSVDHDIYVCLLEDGGSFKSLKRHLTHHSMTPPEYREKWDLPVDYPMVA
M11_Mloti         PEALEPAVPIRKSVPDYIICLDDGKKFKSLKRHLSTHHGLTPDEYRAKWHLPADYPMVA
M15_Mloti         SEALKPAVPIRKSVPDYIISLEDGKKFKSLKRHLATHYGLTPDEYRAKWELPADYPMVA
M13_Mloti         SPSLVPAVNPKKSVPDYIICLEDGKKFKSLKRHLRTDYGLSPDDYRAKWGLPPDYPMVA
M14_Mloti         NPVLTPAVNPKKSVPDYIVSLEDGRKFKSMKRHLG-LLGMTPEYRTKWDLPRDYPMVA
MucR2_Crescentus  PTPKEPAVVPKKSITPDYLI CLEDGKKFKSLKRHLRTKYDMTPEDYRAKWGLPKDYPMVA
MucR1_Crescentus  VVTKATPAQIRKSI TPEALISFEDGKPYKTLKRHLT-THGMTVAEYKAKWGLPNDYPTTA
                  ... : * : : : : * : * : * * * * . : : * : * * * . * * . *

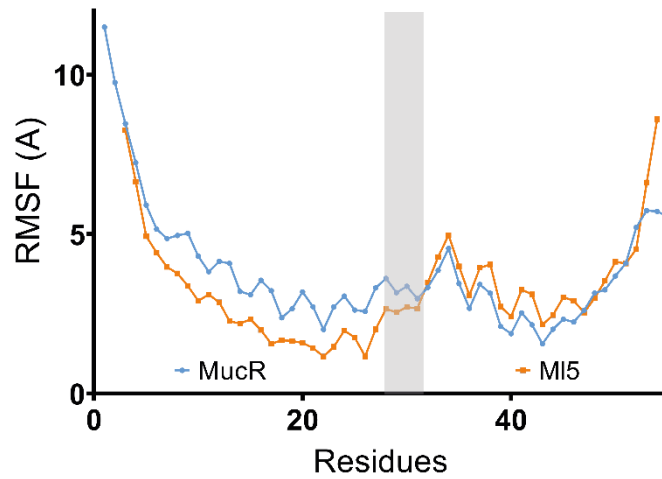
MucR_Babortus      PNYAAARSRLAKKMGLGRKPKDA-----
MucR_Bmelitensis  PNYAAARSRLAKKMGLGRKPKDA-----
M12_Mloti         PNYAAARSRLAKKMGLGRKPKDA-----
MucR_Smeliloti    PAYAEARSRLAKEMGLGQRRKRRGK-----
Ros_Atumefaciens  PAYAEARSRLAKEMGLGQRRKANR-----
M11_Mloti         PNYAAARSALAKTMGLGRKPKPEPEARTRKKA---
M15_Mloti         PNYAAARSALAKTMGLGRKPKPEPETPAPAKRARKKAAA
M13_Mloti         PNYAATRSALAKSTGLGRKPAAPAAVAKKGGKAKA---
M14_Mloti         PNYAATRSALAKASGLGRKAAPVKKAPAKR-KAKA---
MucR2_Crescentus  PNYAEARSNLAKQMGGLGQGRKPKARKAK-----
MucR1_Crescentus  PAYSEARSQMAKALGLGQGRKGTTRGRKG-----
                  * * : * * : * * * * :

```

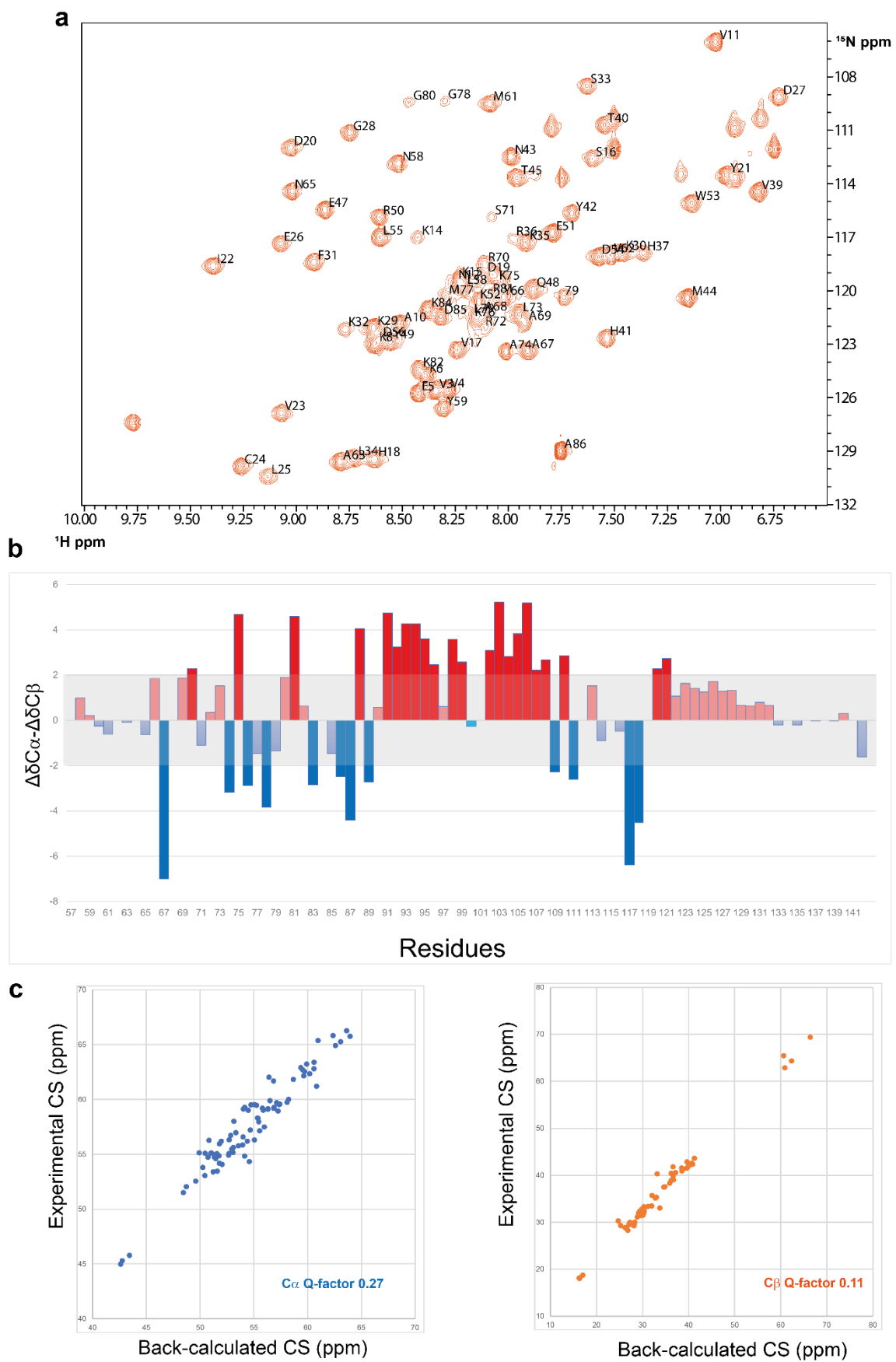
**Supplementary Figure 4.** Sequence alignment (<https://www.genome.jp/tools-bin/clustalw>) of the highly investigated members of Ros/MucR family. Asterisks identify identical residues, dots similar residues. Uniprot accession numbers: Q2YRM3 for *B. abortus* MucR; Q8YFZ8 for *B. melitensis* MucR; Q985J6 for *M. loti* M12; Q04152 for *A. tumefaciens* Ros; Q989W1 for *M. loti* M11; Q98A76 for *M. loti* M15; Q984N1 for *M. loti* M13; Q98DI2 for *M. loti* M14; A0A0H3C684 for *C. crescentus* MucR2; A0A0H3C569 for *C. crescentus* MucR1.



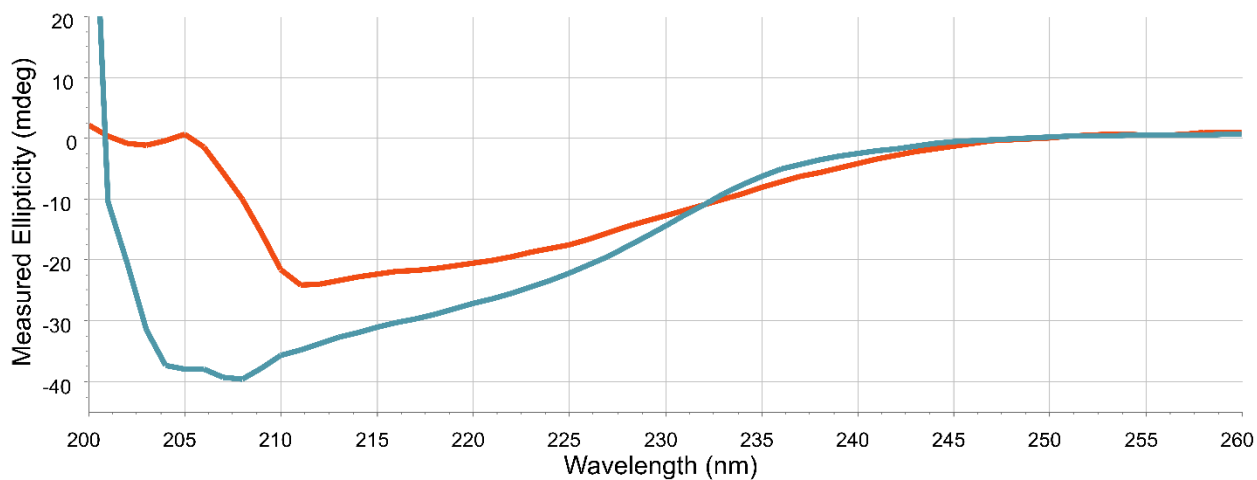
**Supplementary Figure 5.** Upper panel: MucR and MI5 NTDs polarity surfaces. The hydrophobic surface outlined (built by Leu13, Leu15, Leu17, Ala19, Val21, Ala23, Ala24, Ala33, Leu36, Leu39, Ile40, Val43, and Ala46) is responsible for the  $\alpha 1/\alpha 2$  interaction within each monomer and for inter-monomer compaction within the whole assembly of protein particles. The  $\alpha 1$  and  $\alpha 2$  helices are shown in cartoon representation below the transparent protein surface. Lower panel: MucR and MI5 NTDs per-residue hydrophobicity score. Higher score means higher hydrophobicity, lower score indicates higher hydrophilicity.



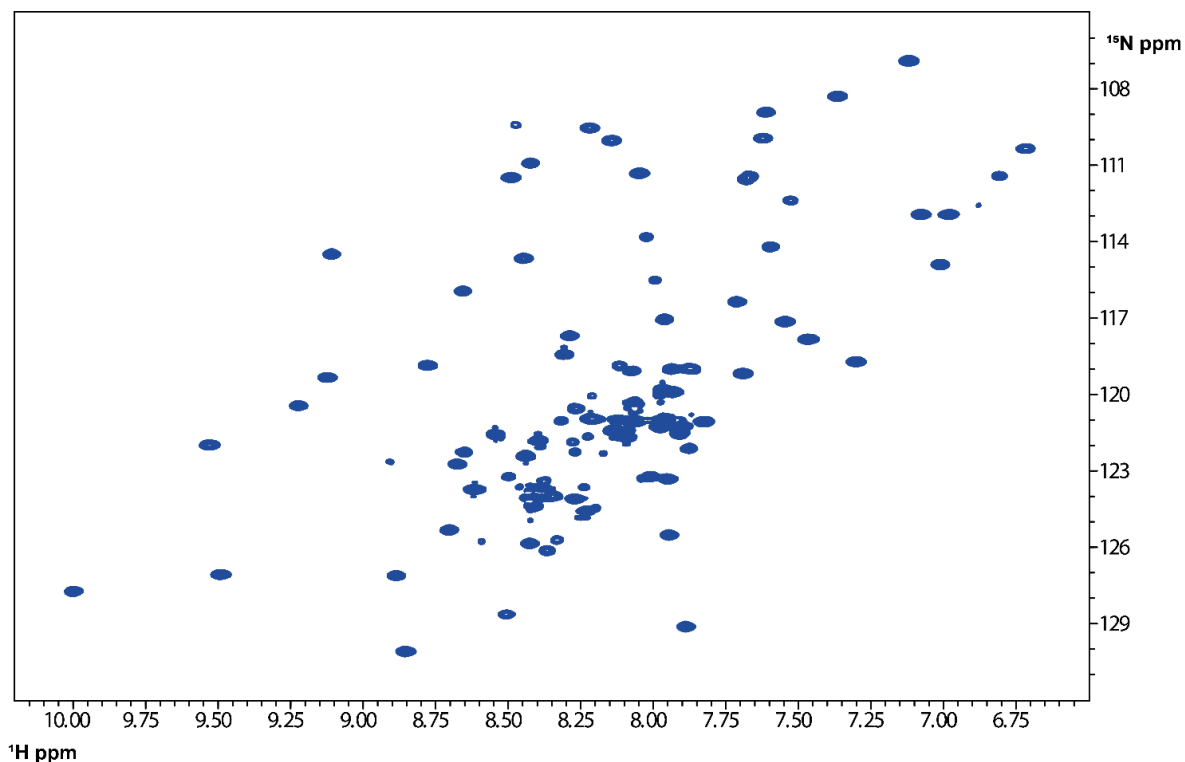
**Supplementary Figure 6.** MucR and MI5 NTDs per-residue C $\alpha$  Root Mean Square Fluctuations (RMSF) determined by NMSim software normal mode analysis. The grey rectangle indicates the linker region between  $\alpha 1$  and  $\alpha 2$  helices. The x-axis scale shows numbering according to the MucR sequence; for MI5 residue numbering, see the alignment in Fig. 1B.



grey area. (c) Plot of experimental  $C\alpha$  (in blue) and  $C\beta$  (in orange) chemical shift correlation versus the same values back-calculated from the AF2 model. The calculated Q-factor is reported in the graph.

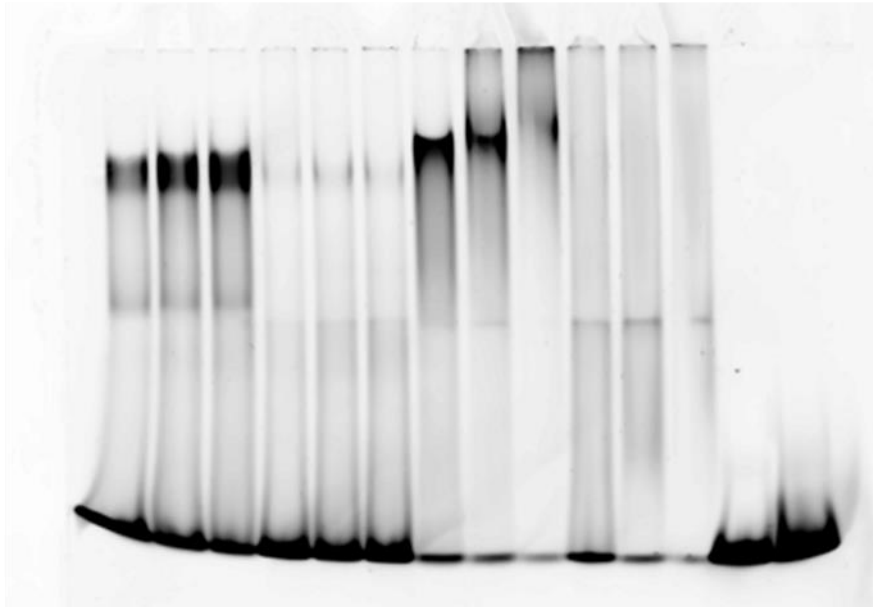


**Supplementary Figure 8.** Far-UV CD spectra of MucR<sub>57-142</sub> (in blue) and apo-MucR<sub>57-142</sub> (in orange).



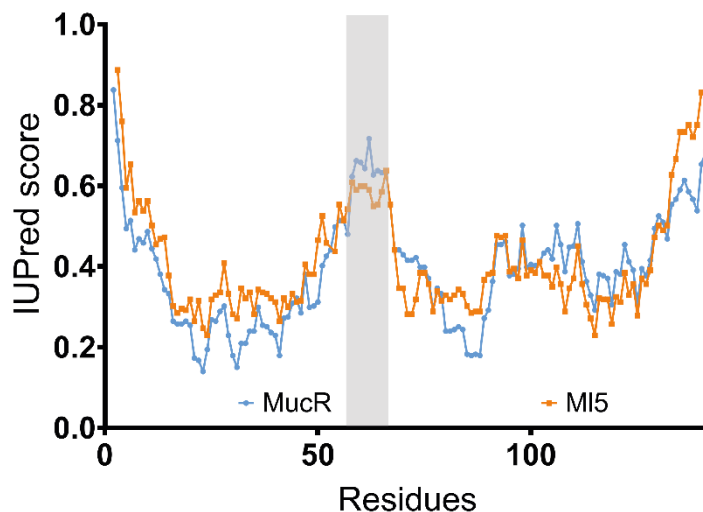
**Supplementary Figure 9.**  $^1\text{H}$ - $^{15}\text{N}$  HSQC spectrum of MI<sub>56-154</sub>.

Target site:	BabR 30 (10 pmol)	NS (10 pmol)	BabR 30 (10 pmol)	NS (10 pmol)	
Protein:	MucR wt (pmol)	MucR wt (pmol)	MI5 wt (pmol)	MI5 wt (pmol)	BabR 30 (10 pmol) NS (10 pmol)
	6 9 12	6 9 12	6 9 12	6 9 12	

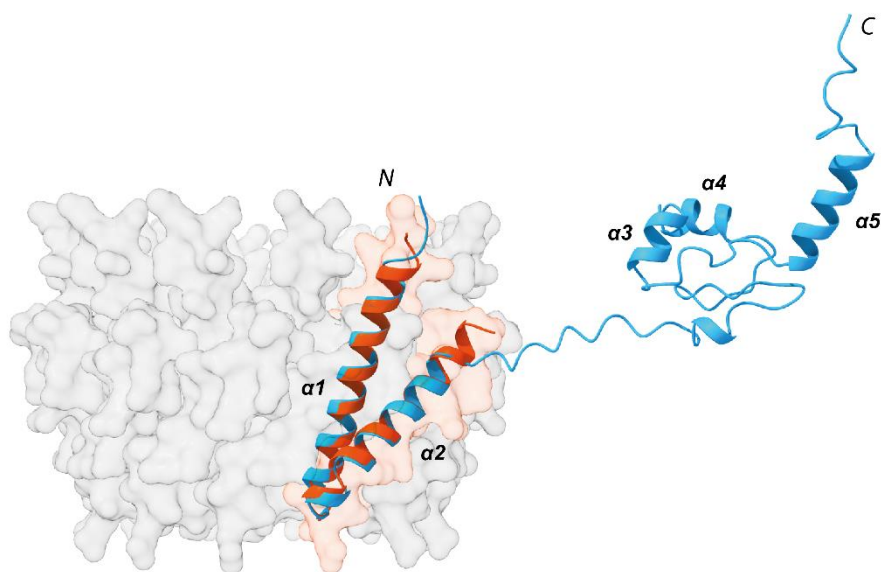


babR30: 5' -ATGAAGTTATATTCAATATAAAAGTAGAAT-3' 83 % AT  
 NS: 5' -CGCGGCACGACCGCAGCGGTCGGGTGGCAC-3' 20 % AT

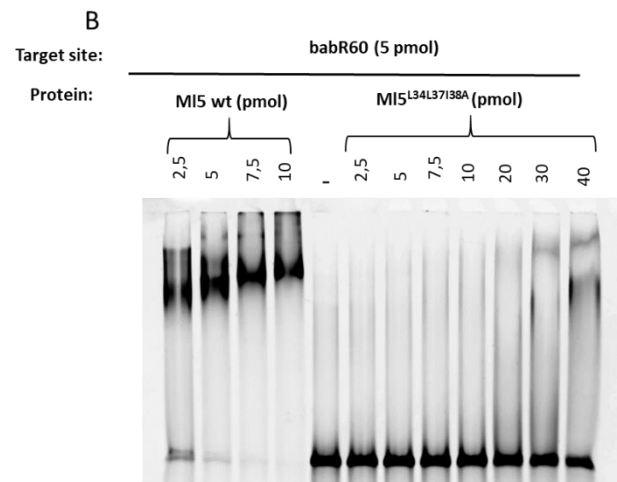
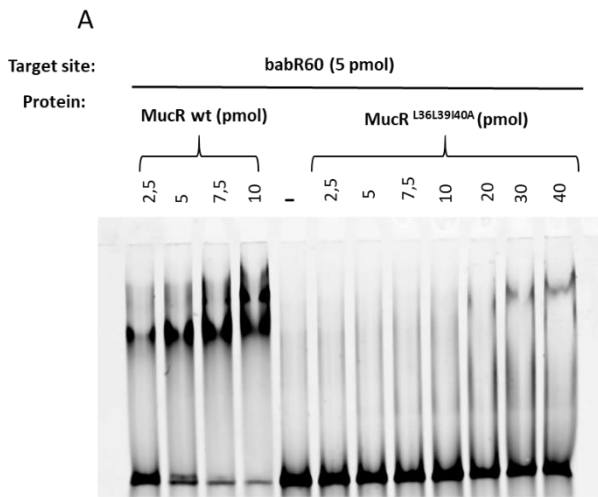
**Supplementary Figure 10:** EMSA with MucR and MI5. The sequences of the two DNA targets used and their AT content are indicated. The sequence of babR30 is derived from the *babR* promoter(1); the NS oligonucleotide was designed as a scrambled GC-rich sequence.



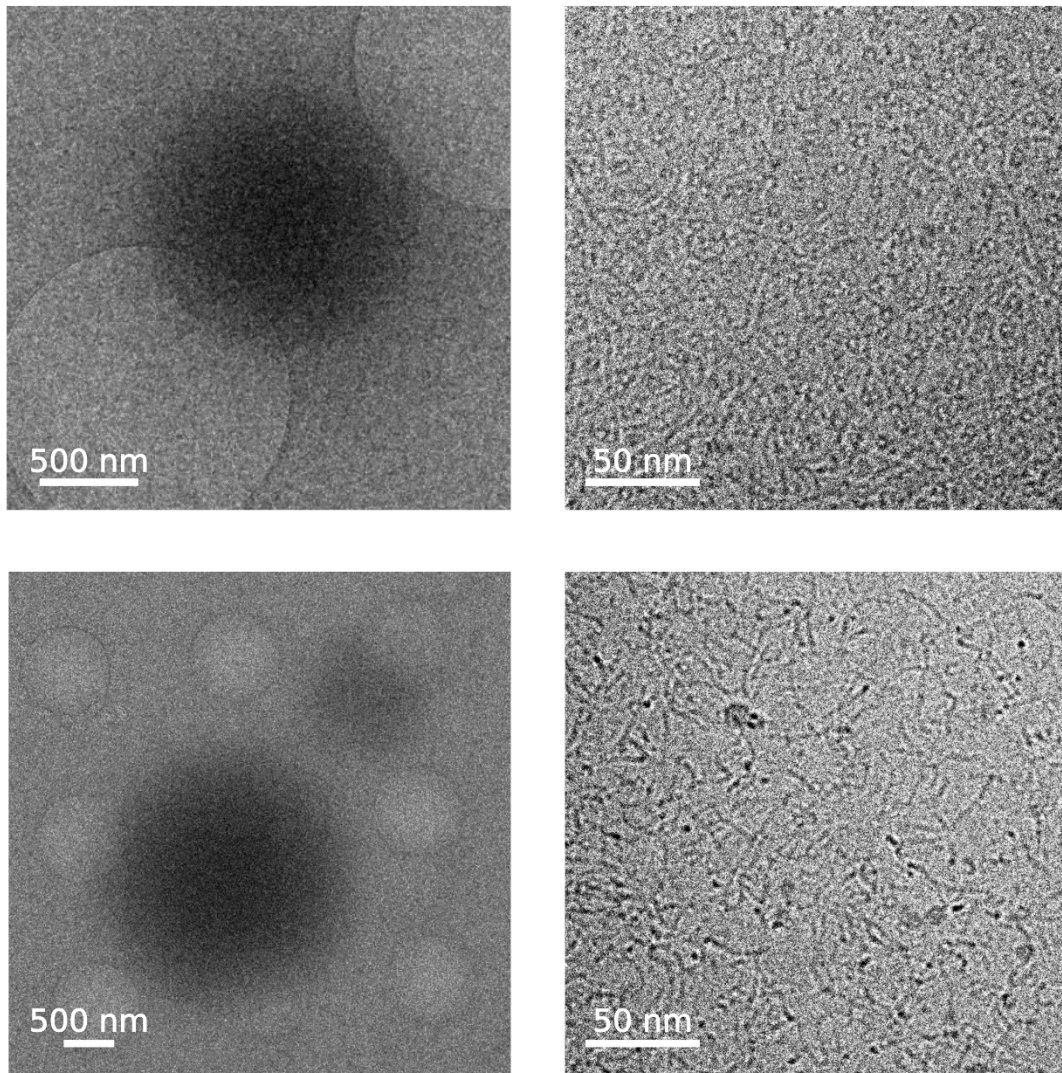
**Supplementary Figure 11.** Per-residue IUPred disorder propensity score of full-length MucR (in blue) and MI5 (in orange). The grey rectangle indicates the linker region between the NTD and DBD. The x-axis scale shows numbering according to the MucR sequence; for MI5 residue numbering, see the alignment in Fig. 1B.



**Supplementary Figure 12.** Superimposition of one protomer of the AF2 model of the MucR NTD dodecameric complex (in red) with the AF model of full-length MucR AF model (in blue). The alignment was made with the  $C\alpha$  of residues 3-52 for both sequences giving an RMSD = 0.7Å.



**Supplementary Figure 13.** EMSA of wild-type MucR, MucR<sup>L36L39I40A</sup>, wild-type MI5 and MI5<sup>L34L37I38A</sup> with the double stranded oligonucleotide babR60(1). The complexes of the two variant proteins with DNA are barely detectable.



**Supplementary Figure 14. Cryo-EM images of MucR-DNA complexes.** Top: Images of MucR in complex with the 232 bp MucR promoter. Bottom: Images of MucR in complex with the 60 bp double stranded oligonucleotide babR60. Both complexes were imaged at low (6.700 x) and high magnification (73.000 x), left and right respectively.

## References

1. Borriello, G., Russo, V., Paradiso, R., Riccardi, M.G., Criscuolo, D., Verde, G., Marasco, R., Pedone, P.V., Galiero, G. and Baglivo, I. (2020) Different Impacts of MucR Binding to the *babR* and *virB* Promoters on Gene Expression in *Brucella abortus* 2308. *Biomolecules*, **10**.

